

# White-Light Emission Strategy of a Single Organic Compound with Aggregation-Induced Emission and Delayed Fluorescence Properties\*\*

Zongliang Xie, Chengjian Chen, Shidang Xu, Jun Li, Yi Zhang,\* Siwei Liu, Jiarui Xu, and Zhenguo Chi\*

**Abstract:** A novel white-light-emitting organic molecule, which consists of carbazolyl- and phenothiazinyl-substituted benzophenone (OPC) and exhibits aggregation-induced emission-delayed fluorescence (AIE-DF) and mechanofluorochromic properties was synthesized. The CIE color coordinates of OPC were directly measured with a non-doped powder, which presented white-emission coordinates (0.33, 0.33) at 244 K to 252 K and (0.35, 0.35) at 298 K. The asymmetric donor–acceptor–donor' (D–A–D') type of OPC exhibits an accurate inherited relationship from dicarbazolyl-substituted benzophenone (O2C, D–A–D) and diphenothiazinyl-substituted benzophenone (O2P, D'–A–D'). By purposefully selecting the two parent molecules, that is, O2C (blue) and O2P (yellow), the white-light emission of OPC can be achieved in a single molecule. This finding provides a feasible molecular strategy to design new AIE-DF white-light-emitting organic molecules.

White-light-emitting organic materials and devices have attracted considerable interest because of their great potential in various lighting applications. Most white-light organic emitters reported thus far rely on a combination of several components that emit different colors of light to completely span the entire visible spectrum.<sup>[1]</sup> Compared with these multicomponent emitters, a single-component white-light organic emitter (that is, a white-light-emitting molecule) exhibits many advantages such as improved stability and reproducibility, as well as a simpler fabrication process.<sup>[2,3]</sup> However, single white-light-emitting molecules are currently limited, and few strategies, if any, for guiding white-light-emitting fluorescence from a single molecule are concluded at the molecular stage.<sup>[3]</sup>

Delayed fluorescence (DF) is a promising approach for converting electricity into light at an internal quantum efficiency of nearly 100%. Thus, DF materials are regarded as the next-generation luminescent materials after fluorescent and phosphorescent materials, and considerable effort has been devoted to their syntheses and investigations.<sup>[4,5]</sup> However, the search for single-component white-light DF materials remains as an urgent challenge, although a multicomponent white-light emitter developed by DF doping technology has been reported recently.<sup>[1d]</sup> Moreover, common DF molecules can easily aggregate through  $\pi$ – $\pi$  interactions, which results in exciton concentration quenching (CQ) caused by singlet–triplet and triplet–triplet annihilations. Thus, these DF molecules can only exhibit efficient DF in doping systems.<sup>[4]</sup>

A significant approach for synthesizing asymmetric D–A–D' type of AIE-DF compounds with efficient triplet harvesting in non-doped solid state was recently reported by our group (SFPC; Figure 1).<sup>[5a]</sup> Afterward, dual-emission SFPC properties were determined by careful characterization. Further investigations focused on analyzing the origin of the dual-emission. Interestingly, the blue and yellow–green emission wavelengths are similar to the emission wavelengths of the parent molecules (SF2C and SF2P; Figure 1).

In the present study, we purposely explored another asymmetric D–A–D' molecule, namely OPC. The component moieties of this molecule came from different parent molecules, namely, O2C and O2P (Figure 1). O2C was selected because its DF molecules were reported as the blueprint of blue emission,<sup>[1d]</sup> and O2P was a model moiety of yellow emission.<sup>[6]</sup> OPC, which is a butterfly-shaped molecule, has blue and yellow emission wings. This molecule is expected to exhibit dual emission because of the parent molecules (O2C and O2P). OPC is found to exhibit AIE-DF nature and white emission in non-doped solid state.

To express the design strategy, our previously reported photoluminescence (PL) spectra of SF2C and SF2P are

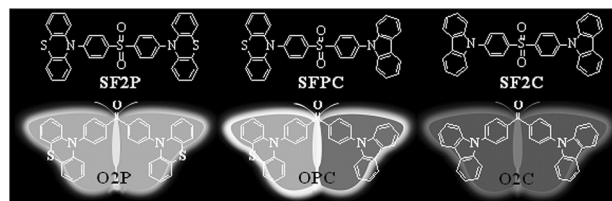


**Figure 1.** Molecular structures of SF2P, SFPC, SF2C, and butterfly-shaped O2P, OPC, and O2C compounds.

[\*] Dr. Z. Xie,<sup>[‡]</sup> Dr. C. Chen,<sup>[‡]</sup> S. Xu, J. Li, Prof. Y. Zhang, Prof. S. Liu, Prof. J. Xu, Prof. Z. Chi  
PCFM Lab and GD HPPC Lab, Guangdong Engineering Technology Research Center for High-performance Organic and Polymer Photoelectric Functional Films, State Key Laboratory of Optoelectronic Material and Technologies, School of Chemistry and Chemical Engineering, Sun Yat-sen University  
Guangzhou 510275 (China)  
E-mail: ceszy@mail.sysu.edu.cn  
chizhg@mail.sysu.edu.cn

[‡] These authors contributed equally to this work.

[\*\*] This work was financially supported from the NSF of China (51173210, 51473185), c863 Programs (SS2015AA031701) and the Fundamental Research Funds for the Central Universities.

Supporting information for this article is available on the WWW under <http://dx.doi.org/10.1002/anie.201502180>.

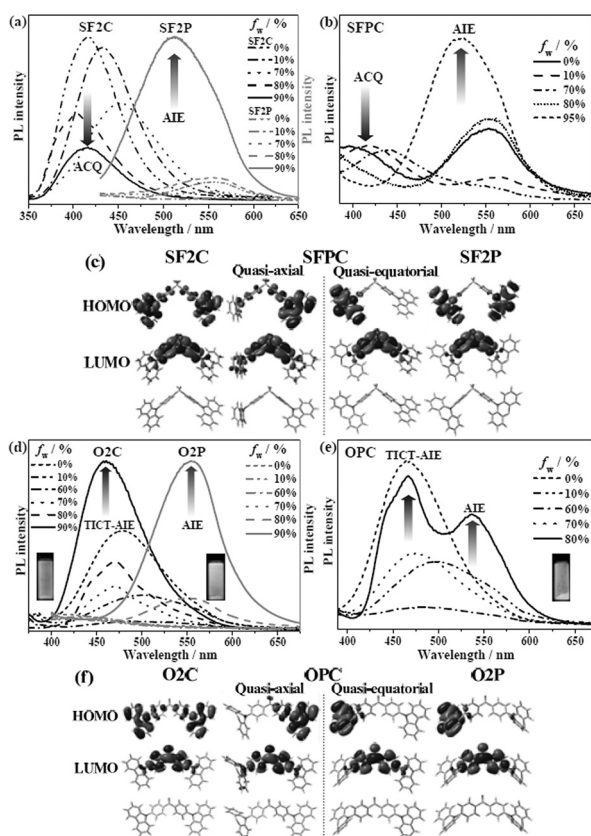


**Figure 2.** PL spectra of a) SF2C and SF2P, b) SFPC, d) O2C and O2P, and e) OPC in tetrahydrofuran (THF)/water mixtures with different  $f_w$ . The HOMO, LUMO, and conformations of c) SF2P, SFPC, and SF2C, and f) O2C, O2P, and OPC were optimized and calculated at B3LYP/6-31G(d,p).

depicted in Figure 2a, and the AIE attribute of SFPC was measured at the same concentration (10.0  $\mu\text{M}$ ). As shown in Figure 2b, SFPC exhibited dual emission; that is, the blue emission demonstrated twisted intramolecular charge transfer (TICT)-CQ behavior with increasing water fraction ( $f_w$ ). Interestingly, its (TICT)-CQ behavior was similar to that of SF2C (Figure 2a, black lines), whereas the yellowish-green emission simultaneously exhibited typical AIE nature, and its PL spectra under different  $f_w$  values were a clone of SF2P (Figure 2a, gray lines).

To confirm the origin of the dual emission of SFPC, the photophysical properties of SF2C, SFPC, and SF2P were further analyzed. Their UV/Vis spectra were measured in toluene solution (Supporting Information, Figure S2a). Interestingly, the absorption spectrum of SFPC showed the characteristic absorptions of both SF2C and SF2P. This observation further indicated a form of molecular inheritance in SFPC from SF2C and SF2P. Compared with the CT absorption of SF2C and SF2P, this result implied that the CT absorption of SFPC is mainly associated with electron transfer from carbazole moiety (C) to sulfobenzide moiety (SF) and from phenothiazine moiety (P) to SF moiety, respectively. Thus, the dual emission wavelengths correspond to the emitted wavelengths of SF2C and SF2P. Accordingly, the dual emission was probably two CT fluorescence.<sup>[7a]</sup> As

shown in the Supporting Information, Figure S2b,c, the transient PL decay curves caused by the oxygen-sensitive behavior and the PL spectra of SFPC and SF2P in toluene are similar. To further confirm this finding, Gaussian09 software was used to calculate the conformers by directly optimizing structures from energy-minimizing and single-crystal structures (Supporting Information, Figures S3 and S4).<sup>[8]</sup> The electron density distributions of the highest occupied molecular orbital (HOMO) and the lowest unoccupied molecular orbital (LUMO) show a remarkable similarity between SF2C and “quasi-axial” SFPC or “quasi-equatorial” SFPC and SF2P (Figure 2c). The anastomotic phenomenon has attracted tremendous interest in tuning dual emission wavelengths to cover the visible range of 400 nm to 700 nm and thus synchronously obtain a single white-light-emitting molecule with a suitable AIE-DF attribute.

Accordingly, two complementary colors (blue/yellow) emissions with an AIE attribute were selected. Based on our previously reported AIE-DF molecules,<sup>[5a]</sup> phenothiazine was introduced to achieve a yellow-emission parent molecule with AIE attributes. The challenge to obtain blue-emission parent molecule with an AIE attribute was solved by introducing carbazole, which was frequently used to produce blue AIE materials.<sup>[9]</sup>

As shown in Figure 2d ( $f_w$ : 0% to 60%, black lines), O2C exhibited TICT, which was featured with a red-shifted emission and weakened emission intensity with increasing solvent polarity.<sup>[10]</sup> Light emission was intensified after 60% of  $f_w$ , and the maximum emission was blue-shifted to 460 nm at 90%. That is, the TICT-AIE properties of O2C indicated its potential as a blue-emission source in solid state. As shown in Figure 2d (gray line), the spectral profile was virtually unchanged with increasing  $f_w$  of 0% to 70%. Emission intensity was sharply enhanced after 80% of  $f_w$  and the maximum wavelength was 554 nm at 90%. These typical AIE properties implied that O2P succeeded in performing a yellow-emission parent molecule function.

As predicted, OPC exhibited a TICT-AIE attribute at the blue-emission region (Figure 2e), which was retained from the TICT-AIE of its parent form, that is, O2C.<sup>[10]</sup> Analogously, the maximum emission of the blue-emission region was blue-shifted to 467 nm at 80%. The AIE attribute of OPC was further measured in a dilute concentration (Supporting Information, Figure S5). The yellow-emission region of OPC exhibited typical AIE properties, and the emission maximum was 552 nm at 95% (Supporting Information, Figure S5). Consequently, the dual-emission OPC with AIE properties at both the blue- and yellow-emission regions was successfully developed. Meanwhile, pure white emission was also produced (Supporting Information, Figure S1 with an inset of Figure 2e). Furthermore, the CIE coordinates were measured (0.35, 0.35) with a solid powder at room temperature.

To illustrate the strategy further, UV/Vis and PL spectra were measured (Supporting Information, Figure S2d–f). Furthermore, the electron-density distributions of the HOMO and the LUMO were calculated (Figure 2f). The results further indicated that the white-light emission strategy was completely developed in D-A-D' type.

With a goal-directed DF design,  $\Delta E_{ST}$  values were calculated at the B3LYP/6-31G\* level. The O2C value was reported to be 0.32 eV, and DPEPO was selected as the host to produce DF.<sup>[1d]</sup> The newly calculated values of “quasi-axial” OPC, “quasi-equatorial” OPC, and O2P were 0.56, 0.01, and 0.01 eV, respectively. These results suggested a nearly prohibited reverse intersystem crossing (RISC) in “quasi-axial” OPC, and by contrast a potentially efficient RISC in “quasi-equatorial” OPC and O2P.

In general, the up-conversion of triplet excitons that are necessary to produce DF can be characterized by transient PL decay curves and further confirmed by oxygen-sensitive behavior with PL spectra.<sup>[4,5]</sup> Given that O2P and OPC exhibited AIE attributes, DF was simultaneously measured in solution and in non-doped solid powder. As shown in Figure 3a and b, an increasing single-exponential lifetime of DF ranging from 14 ns to 86 ns for O2P and 16 ns to 75 ns for the yellow emission of OPC at 300 K was observed after oxygen degassing by nitrogen. This observation indicated that a typical oxygen-sensitive behavior in toluene solution was characterized, and the corresponding PL spectra are shown in the insets.

Notably, the transient PL decay curves of O2P and the yellow emission of OPC were multi-exponential decays in the solid state (Figure 3c and d). A similar discovery was recently reported and explained with b3 in doped CBP films by Adachi.<sup>[4b]</sup> These findings implied that multi-exponential decays may result from different rotamers in solid state.<sup>[4b,5]</sup> To confirm the DF, the results are amplified in the insets of Figure 3c and d, which presented remarkable temperature

dependence with increasing DF from 77 K to 300 K.<sup>[4]</sup> Furthermore, the evident oxygen-sensitive PL spectra in non-doped solid state were measured (Figure 3e and f). These findings indicated that  $T_1$  excitons could be deactivated by triplet oxygen in the solid state. By contrast, efficient RISC was further maintained by AIE properties from the solution to the solid state, which demonstrated various application fields by breaking doping restrictions.<sup>[5]</sup> Accordingly, the overall fluorescence efficiency ( $\Phi_F$ ) of O2P (13.9%, in air) and OPC (23.3%, in air) were underestimated. Meanwhile, as predicted by their  $\Delta E_{ST}$  values, the DF of O2C and the blue light of OPC in non-doped solid state was not observed (Figure 3d and f; Supporting Information, Figure S6). Thus, blue emission was confirmed to be normal AIE fluorescence. Based on the preceding observations, O2P and O2C exhibited an accurate inherited relationship in OPC. That is, O2C demonstrated normal AIE fluorescence in non-doped solid state (Supporting Information, Figure S6), and O2P presented AIE-DF. Correspondingly, the blue and yellow emissions of OPC were confirmed to be normal AIE fluorescence and AIE-DF, respectively.

As mentioned, the 460 nm emission in the non-doped solid state of OPC was normal AIE fluorescence, which increased PL intensity with decreasing temperature.<sup>[9a,b]</sup> However, the 580 nm emission was proven to be a typical AIE-DF, which presented different temperature dependence degrees.<sup>[5]</sup> Accordingly, the temperature dependence of PL characteristics was determined (Figure 4a). Interestingly, the PL intensity of yellow emission was nearly stable, which was mainly ascribed to DF. Consequently, white emission (0.35, 0.35) at room temperature from OPC could be tuned to a pure white emission with decreasing temperature. The corresponding CIE coordinates were calculated and shown in Figure 4b. Considering the AIE attribute, the CIE coordinates of OPC were further measured in non-doped solid state and presented

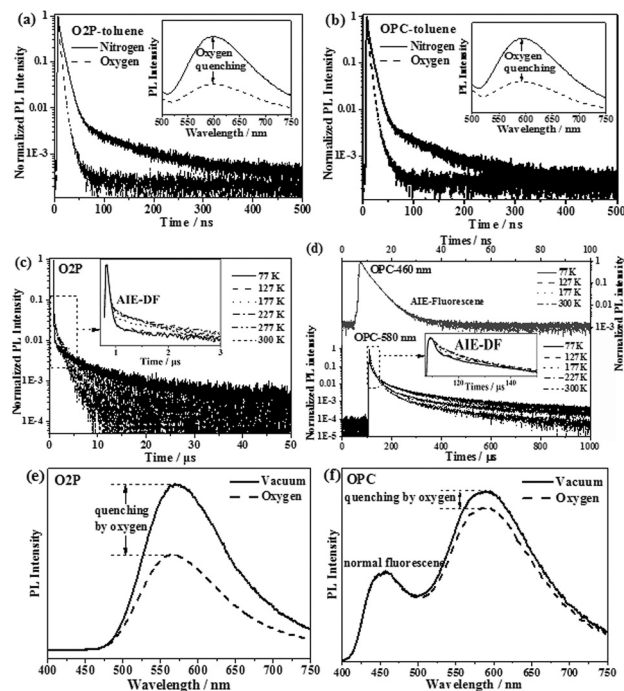


**Figure 3.** Transient PL decay curves of a) O2P and b) OPC in toluene solution (10.0  $\mu$ M). Temperature dependence of transient PL decay curves of c) O2P and d) OPC in the non-doped solid state. e), f) PL spectra of vacuum/oxygen. Insets of (a) and (b) depict PL spectra of nitrogen/oxygen in toluene solution.

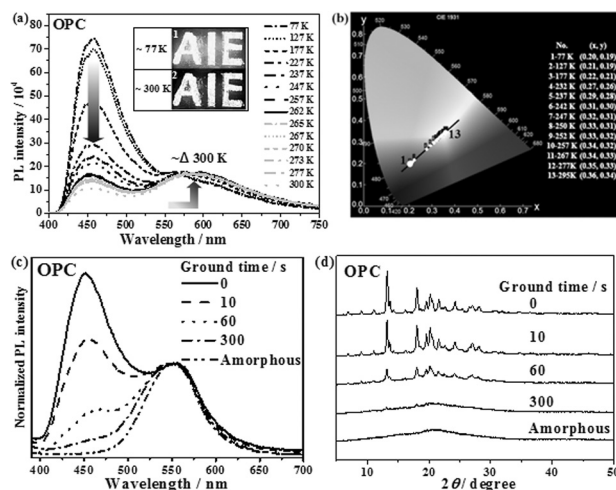


**Figure 4.** a) PL spectra of OPC in non-doped solid state with temperature increasing from 77 K to 300 K and b) calculated PL emission color coordinates in the CIE 1931 chromaticity diagram. c) PL spectra and d) corresponding XRD of OPC in the solid state with different grounding time and its amorphous state. Insets of (a): images 1) in liquid nitrogen and 2) at room temperature.



(0.32, 0.32) at 234 K to (0.35, 0.35) at 298 K with (0.33, 0.33) at 244 K to 252 K. In general, the AIE fluorescence is stable before glass transition temperature ( $T_g$ ) is reached. The thermal properties of OPC were measured ( $T_g = 97^\circ\text{C}$ ; Supporting Information, Figure S7).

To further understand dual emission from two ground-state conformations, the mechanical stimulus of grinding was used to break the balance.<sup>[11]</sup> The PL characteristics and XRD were used for analysis (Figure 4c and d). The original OPC showed a dual emission of 456 nm and 554 nm and the crystalline component was gradually obliterated with increasing grinding time, whereas the corresponding PL intensity of blue emission simultaneously declined, which indicated that OPC was also a mechanofluorochromic compound.<sup>[11a]</sup> Accordingly, the blue emission of 456 nm was ascribed to a crystallographic state, which probably exhibited “quasi-axial” conformer (Supporting Information, Figures S3 and S6).<sup>[7]</sup> Furthermore, the yellow emission of 554 nm was attributed to an amorphous state, which probably adopted “quasi-equatorial” conformer. Interestingly, the two ground-state conformations of phenothiazine derivatives probably sequentially coexisted at equal proportions in solid state because the two conformers of PTZ-TRZ differed only by 0.02 eV and 0.06 eV for SFPC and 0.04 eV for OPC (Supporting Information, Figure S4).<sup>[7a]</sup>

In conclusion, according to the strategy of our previously reported systems of D-A-D (SF2C, doped DF), D-A-D' (SFPC, AIE-DF), and D'-A-D' (SF2P, AIE-DF) molecules, we produced a single white-light-emitting AIE-DF molecule, namely OPC, with a constant phenathazine donor. The molecular design strategy proved its feasibility. OPC and O2P were established as new types of rare AIE-DF molecules that generate both white and yellow emissions in non-doped solid state. Furthermore, dual emission was successfully developed with the D-A-D' type, which presented a novel strategy for tuning luminescence by properly selecting parent molecules (that is, D-A-D and D'-A-D'). Single white-light-emitting DF molecules exhibited considerable significance for future display and lighting applications. Furthermore, this design strategy provides a novel direction for producing white-light organic compounds. OPC also exhibits a unique mechanofluorochromic nature. Further design and synthesis of new single white-light-emitting DF molecules are currently being developed using the proposed strategy.

**Keywords:** aggregation-induced emission · delayed fluorescence · dual emission · white-light emission

**How to cite:** *Angew. Chem. Int. Ed.* **2015**, *54*, 7181–7184  
*Angew. Chem.* **2015**, *127*, 7287–7290

- [1] a) J. Kido, M. Kimura, K. Nagai, *Science* **1995**, *267*, 1332–1334; b) Y. Sun, N. C. Giebink, H. Kanno, B. Ma, M. E. Thompson, S. R. Forrest, *Nature* **2006**, *440*, 908–912; c) S. Reineke, F. Lindner, G. Schwartz, N. Seidler, K. Walzer, B. Lüssem, K. Leo, *Nature* **2009**, *459*, 234–238; d) S. Y. Lee, T. Yasuda, Y. S. Yang, Q. Zhang, C. Adachi, *Angew. Chem. Int. Ed.* **2014**, *53*, 6402–6406; *Angew. Chem.* **2014**, *126*, 6520–6524; e) K. V. Rao, K. K. R. Datta, M. Eswaramoorthy, S. J. George, *Adv. Mater.* **2013**, *25*, 1713–1718.
- [2] a) Y. Liu, M. Nishiura, Y. Wang, Z. Hou, *J. Am. Chem. Soc.* **2006**, *128*, 5592–5593; b) Q. Y. Yang, J. M. Lehn, *Angew. Chem. Int. Ed.* **2014**, *53*, 4572–4577; *Angew. Chem.* **2014**, *126*, 4660–4665; c) M. Han, Y. Tian, Z. Yuan, L. Zhu, B. Ma, *Angew. Chem. Int. Ed.* **2014**, *53*, 10908–10912; *Angew. Chem.* **2014**, *126*, 11088–11092; d) S. H. Kim, S. Park, J. E. Kwon, S. Y. Park, *Adv. Funct. Mater.* **2011**, *21*, 644–651.
- [3] a) S. Shao, J. Ding, L. Wang, X. Jing, F. Wang, *J. Am. Chem. Soc.* **2012**, *134*, 20290–20293; b) K. T. Kamtekar, A. P. Monkman, M. R. Bryce, *Adv. Mater.* **2010**, *22*, 572–582; c) S. Park, J. E. Kwon, S. H. Kim, J. Seo, K. Chung, S. Y. Park, D. J. Jang, B. M. Medina, J. Gierschner, S. Y. Park, *J. Am. Chem. Soc.* **2009**, *131*, 14043–14049; d) J. Y. Li, D. Liu, C. Ma, O. Lengyel, C. S. Lee, C. H. Tung, S. T. Lee, *Adv. Mater.* **2004**, *16*, 1538–1541.
- [4] a) H. Uoyama, K. Goushi, K. Shizu, H. Nomura, C. Adachi, *Nature* **2012**, *492*, 234–238; b) Q. Zhang, H. Kuwabara, W. J. Potscavage, Jr., S. Huang, Y. Hatae, T. Shibata, C. Adachi, *J. Am. Chem. Soc.* **2014**, *136*, 18070–18081; c) H. Nakanotani, K. Masui, J. Nishide, T. Shibata, C. Adachi, *Sci. Rep.* **2013**, *3*, 2127; d) G. Méhes, H. Nomura, Q. Zhang, T. Nakagawa, C. Adachi, *Angew. Chem. Int. Ed.* **2012**, *51*, 11311–11315; *Angew. Chem.* **2012**, *124*, 11473–11477; e) F. B. Dias, K. N. Bourdakos, V. Jankus, K. C. Moss, K. T. Kamtekar, V. Bhalla, J. Santos, M. R. Bryce, A. P. Monkman, *Adv. Mater.* **2013**, *25*, 3707–3714; f) H. Nakanotani, T. Higuchi, T. Furukawa, K. Masui, K. Morimoto, M. Numata, H. Tanaka, Y. Sagara, T. Yasuda, C. Adachi, *Nat. Commun.* **2014**, *5*, 4016.
- [5] a) S. Xu, T. Liu, Y. Mu, Y. F. Wang, Z. Chi, C. C. Lo, S. Liu, Y. Zhang, A. Lien, J. Xu, *Angew. Chem. Int. Ed.* **2015**, *54*, 874–878; *Angew. Chem.* **2015**, *127*, 888–892; b) H. Wang, L. Xie, Q. Peng, L. Meng, Y. Wang, Y. Yi, P. Wang, *Adv. Mater.* **2014**, *26*, 5198–5204; c) J. Li, Y. Jiang, J. Cheng, Y. Zhang, H. Su, J. W. Y. Lam, H. H. Y. Sung, K. S. Wong, H. S. Kwok, B. Z. Tang, *Phys. Chem. Chem. Phys.* **2015**, *17*, 1134–1141.
- [6] C. Chen, J. Y. Liao, Z. Chi, B. Xu, X. Zhang, D. B. Kuang, Y. Zhang, S. Liu, J. Xu, *J. Mater. Chem.* **2012**, *22*, 8994–9005.
- [7] a) H. Tanaka, K. Shizu, H. Nakanotani, C. Adachi, *J. Phys. Chem. C* **2014**, *118*, 15985–15994; b) J. Daub, R. Engl, J. Kurzawa, S. E. Miller, S. Schneider, A. Stockmann, M. R. Wasielewski, *J. Phys. Chem. A* **2001**, *105*, 5655–5665; c) A. Stockmann, J. Kurzawa, N. Fritz, N. Acar, S. Schneider, J. Daub, R. Engl, T. Clark, *J. Phys. Chem. A* **2002**, *106*, 7958–7970; d) N. Acar, J. Kurzawa, N. Fritz, A. Stockmann, C. Roman, S. Schneider, T. Clark, *J. Phys. Chem. A* **2003**, *107*, 9530–9541.
- [8] Gaussian09 (Revision B.01), M. J. Frisch, et al., Gaussian Inc., Wallingford CT, **2009**.
- [9] a) Z. Yang, Z. Chi, T. Yu, X. Zhang, M. Chen, B. Xu, S. Liu, Y. Zhang, J. Xu, *J. Mater. Chem.* **2009**, *19*, 5541–5546; b) B. Xu, Z. Chi, Z. Yang, J. Chen, S. Deng, H. Li, X. Li, Y. Zhang, N. Xu, J. Xu, *J. Mater. Chem.* **2010**, *20*, 4135–4141; c) X. Zhang, Z. Chi, H. Li, B. Xu, X. Li, S. Liu, Y. Zhang, J. Xu, *J. Mater. Chem.* **2011**, *21*, 1788–1796.
- [10] a) W. Qin, D. Ding, J. Liu, W. Z. Yuan, Y. Hu, B. Liu, B. Z. Tang, *Adv. Funct. Mater.* **2012**, *22*, 771–779; b) W. Qin, K. Li, G. Feng, M. Li, Z. Yang, B. Liu, B. Z. Tang, *Adv. Funct. Mater.* **2014**, *24*, 635–643; c) R. Hu, E. Lager, A. Aguilar-Aguilar, J. Liu, J. W. Y. Lam, H. H. Y. Sung, I. D. Williams, Y. Zhong, K. S. Wong, E. Peña-Cabrera, B. Z. Tang, *J. Phys. Chem. C* **2009**, *113*, 15845–15853.
- [11] a) Z. Chi, X. Zhang, B. Xu, X. Zhou, C. Ma, Y. Zhang, S. Liu, J. Xu, *Chem. Soc. Rev.* **2012**, *41*, 3878–3896; b) K. Wang, H. Zhang, S. Chen, G. Yang, J. Zhang, W. Tian, Z. Su, Y. Wang, *Adv. Mater.* **2014**, *26*, 6168–6173.

Received: March 8, 2015

Published online: April 29, 2015